An Efficient Signal Acquisition with an Adaptive Rate A/D Conversion

Saeed Mian Qaisar[1], Reda Yahiaoui[2], Tijani Gharbi[1]
[1]Nanomedicine Laboratory, 16 Route de Gray, 25030 Cedex Besançon, France
[1]{saeed.mian_qaisar, tijani.gharbi}@univ-fcomte.fr, [2]reda.yahiaoui@femto-st.fr

***Abstract*—The analog to digital conversion is an elementary part of the modern electronic systems. Almost all existing ADCs (Analog to Digital Converters) are based on the uniform sampling theory. It makes the signal acquisition time-invariant. Therefore, it can render a useless increase of the system activity, especially in the case of sporadic signals. Thus, an adaptive rate ADC which is based on the cross-level sampling is devised. It can adapt its conversion activity according to the input signal local variations. Therefore, it provides an intelligent signal acquisition which leads towards an efficient solution. The proposed ADC performance is studied for a speech acquisition. Results show a drastic reduction in the acquired number of samples and therefore promise a significant enhancement in the system power efficiency compared to the classical approach. A method to measure the proposed converter resolution is described. Moreover, its design flow is also presented.**

Keywords- Compression gain, Adaptive rate A/D conversion, Effective resolution, Cross-level sampling.

I. INTRODUCTION

THE motivation of this work is to achieve an intelligent signal acquisition. The idea is to adapt the ADC conversion frequency by following the input signal local characteristics. The existing ADCs are based on the uniform sampling and processing theory. They do not exploit the signal local variations and sample it at a fixed rate without taking into account its intrinsic nature [1]. Due to this time-invariant nature they are parameterized for the worst case. Thus, they are highly constrained especially in the case of low activity sporadic signals like electrocardiogram, phonocardiogram, seismic etc. It causes to capture and therefore to process a large number of samples without any relevant information, a useless increase of the overall system power consumption.

In this article, this shortcoming is treated up to a certain extent by employing an ARADC (Adaptive Rate ADC), which is based on the LCSS (Level Crossing Sampling Scheme) [2]. The LCSS adapts its sampling rate according to the input signal local characteristics [3]. Hence, it drastically reduces the activity of the post processing chain, because it only samples the relevant information [5, 6]. In recent years, the LCSS is employed in a variety of contexts [1-13].

II. THE ARADC (ADAPTIVE RATE ADC)

The ARADC block diagram is shown in Figure 1. Details of the ARADC different stages are given in the following subsections.

A. The LCADC (LCSS based ADC)

In the ARADC, a band-limited analog signal $x(t)$ is digitized with a LCADC [7-9]. The sampling instants of a non-uniformly sampled signal obtained with the LCADC are defined by Equation 1 [2]. Where, t_n is the current sampling instant, t_{n-1} is the previous one and dt_n is the time delay between the current and the previous sampling instants.

$$t_n = t_{n-1} + dt_n . \tag{1}$$

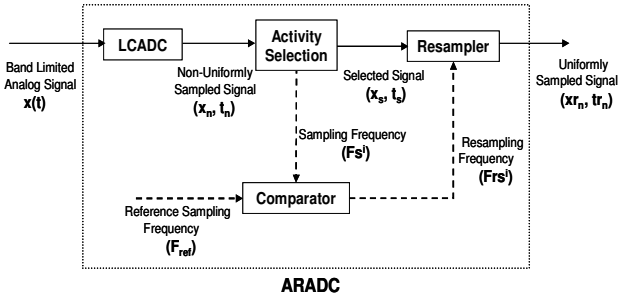

Fig. 1. The ARADC block diagram.

B. Activity Selection

The LCADC delivers a non-uniform time repartitioned output. One drawback of LCADCs is that the relevant signal parts can be locally sampled at higher rates compared to the classical case [7, 12]. In the proposed approach, this shortcoming is treated by exploiting the level crossing sampled signal non-uniformity. It yields information on the signal local features. This information is employed to select only the relevant signal parts. Furthermore, characteristics of each selected part are analyzed and are employed to adapt the system resampling frequency accordingly. It enables resampling the selected data at the same or lower rates compared to the classical approach and therefore renders into a drastic processing efficiency compared to the classical case [6, 11, 13, 17]. This selection and local-features extraction process is named as the activity selection [5, 10].

The LCADC sampling frequency is correlated to $x(t)$ local variations [7, 13, 17]. Let W^i represents the i^{th} selected window, obtained with the activity selection [5, 10]. If Fs^i represents the LCADC sampling frequency for W^i, then, it can be calculated by employing Equation 2. Where, L^i is the length in seconds and N^i is the number of samples laying in W^i.

$$Fs^i = \frac{N^i}{L^i}. \tag{2}$$

The activity selection process displays interesting features with the LCADC, which are not available in the classical case. It selects only the relevant parts of the non-uniformly sampled signal, obtained with the LCADC. Moreover, it correlates the selected window length with the signal local features. In addition, it provides an efficient reduction of the spectral leakage phenomenon [5, 10].

C. Resampler

The selected signal obtained with the activity selection process is resampled uniformly (cf. Figure 1). The resampler acts as a bridge between the non-uniform and the uniform signal processing domains. It enables to take advantage of both sides signal processing tools, in order to achieve smart solutions [5, 6, 10, 11, 13, 17].

Let Frs^i be the resampling frequency for W^i, then its choice

depends on F_{ref} and Fs^i. Here, F_{ref} is the chosen reference sampling frequency in the system, such as it remains greater than and closest to $F_{Nyq}=2.f_{max}$. Here, f_{max} is the input signal bandwidth. After resampling, there exist Nr^i samples for W^i.

For the case, $Fs^i>F_{ref}$, Frs^i is chosen as: $Frs^i=F_{ref}$. It makes to resample W^i closer to the Nyquist rate, so avoids unnecessary interpolations during the data resampling process. Thus, it improves the proposed approach power efficiency. Otherwise, when $Fs^i \leq F_{ref}$, Frs^i is chosen as: $Frs^i=Fs^i$. In this case, it appears that Frs^i may be lower than the Nyquist frequency of $x(t)$ and so it can cause aliasing. According to [6, 11], for the considered signal statistics an appropriate choice of the LCADC dynamic range ΔV_{in} and resolution M can be made. It makes the signal to cross enough consecutive thresholds. Thus, it is locally oversampled with respect to its local bandwidth and so there is no aliasing problem [6, 11].

III. The ARADC Effective Resolution

The practically achievable ADC resolution is known as its effective resolution. It is measured in terms of bits and is defined as the *ENOB* (Effective Number of Bits) [14, 15]. The different ARADC stages are shown in Figure 1. Each stage has its impact on the overall *ENOB*. The error sources and methods to compute the *SNR* (Signal to Noise Ratio) at different ARADC stages are described in the following subsections.

A. The LCADC SNR

The theoretical *SNR* of the classical and the level crossing ADCs can be expressed by Equations 3 and 4 respectively [7-9, 13-15].

$$SNR\,(dB) = 6.02\,M + 1.76. \tag{3}$$

$$SNR\,(dB) = -11.19 - 20.\log\left(f_{sig}.T_{Timer}\right). \tag{4}$$

In Equation 3, M is the ADC number of bits. It follows that the *SNR* of an ideal ADC depends only on M and it can be improved by 6.02 dB for each increment in M.

In Equation 4, f_{sig} is the input signal frequency. In this case, the *SNR* does not depend on M any more, but on $x(t)$ characteristics and T_{timer} [7, 8]. Here, T_{timer} is the timer step used to record the level crossing instants. Theoretically, an improvement of 6.02 dB in the *SNR* can be achieved by simply halving T_{timer} [7-9

Because of the system implementation limitations like the time jitter, the comparators ambiguity etc. the ADC practical SNR_{real} is lower than the theoretical one. In practice, the SNR_{real} is measured from the spectrum of a windowed sequence of the ADC output samples [14, 15]. By knowing the SNR_{real} of an ADC, its *ENOB* can be calculated by employing the following Equation [14, 15].

$$ENOB = \frac{SNR_{real}\,(dB) - 1.76}{6.02}. \tag{5}$$

The LCADC output is non-uniformly distributed in time. Hence, its spectrum can not be properly computed with the classical tools. Although several methods have been developed for computing the non-uniformly sampled signals spectra, yet they are not error free for the LCSS [5]. Thus, they can not provide a proper calculation of the LCADC SNR_{real}. In this context, a novel approach has been proposed for the LCADC SNR_{real} measurement [13]. It does not require frequency domain transformation and calculates the SNR_{real} in time domain.

In practice, a classical ADC is usually characterized by employing a monotone sinusoid [14, 15]. Therefore, a similar signal is employed in the proposed case. For a mono harmonic signal, it is possible to analytically calculate the level crossing instants [3, 13]. In this case, t_n can be calculated by employing Equation 6. Where, f_{sig} and A are the input sinusoid frequency and amplitude. $level_m$ is the m^{th} level crossing threshold. The corresponding amplitude of the n^{th} level crossing sample x_n is given as: $x_n=level_m$. By employing this method, firstly an ideal LCSS is implemented for $x(t)$.

$$t_n = \frac{1}{2\pi f_{sig}}.\arcsin\left(\frac{level_m}{A}\right). \tag{6}$$

The only error occurs in the ideal LCADC is the time quantization [7-9]. By assuming that the time error is uncorrelated to the input signal, it is modeled as a white noise. If δt_n is the time quantization occurs for t_n, then it can randomly takes a value between [0; T_{timer}[, [13]. Thus, tq_n (the quantized t_n version) can be obtained with Equation 7. The time quantization also affects the amplitude value of the corresponding level crossing sample [13]. The erroneous sample amplitude is given by Equation 8.

$$tq_n = t_n + \delta t_n. \tag{7}$$

$$xq_n = A.Sin\left(2\pi.f_{sig}.tq_n\right). \tag{8}$$

For a real LCADC, there also exists error due to the threshold levels ambiguity [7, 8]. Let Δa_n is the error introduced into xq_n due to the threshold levels ambiguity. Then, the n^{th} erroneous level crossing sample amplitude xe_n, can be calculated by employing Equation 9. The real LCADC conversion error per sample point Ce_n is given by the absolute difference between x_n and xe_n. The *RMS* (root mean square) of the LCADC conversion error for W^i is given by Equation 10. Finally, the LCADC SNR_{real} can be calculated as a ratio between the RMS (signal) and the RMS (*Ce*).

$$xe_n = xq_n \pm \Delta a_n. \tag{9}$$

$$RMS\,(Ce) = \sqrt{\frac{1}{N^i}.\sum_{n=1}^{N^i} Ce_n{}^2}. \tag{10}$$

B. The Activity Selection SNR

For a monotone sinusoid, the activity selection algorithm parameters can be easily adjusted to avoid the signal truncation [5, 10]. In this case, the windowing is performed with an adaptive length rectangular function [5, 10]. Hence, it does not introduce any imprecision at the LCADC output [13].

C. Resampler SNR

The resampler requires interpolation, which changes the resampled signal properties compared to the original one [16]. The interpolation error is a function of the employed interpolator order (I^O) and the LCADC resolution M [13, 17In reality, there exist uncertainties in the time-amplitude pairs of the level-crossing samples. These uncertainties accumulate in the interpolation process and deliver the overall error at the ARADC output.

If Ie_n is the error per interpolated observation, then it is given by the absolute difference between xo_n and xr_n. Here, xr_n is the n^{th} resampled observation, interpolated with respect to the time instant tr_n, xo_n is the original sample value which should be obtained by sampling $x(t)$ at tr_n. The *RMS* of the resampling error for W^i is given by Equation 11. Hence, the ARADC SNR_{real} can be calculated as a ratio between the RMS (signal) and the RMS (*Ie*). Finally, the ARADC *ENOB* can be computed by employing Equation 5, [13].

$$RMS\,(Ie) = \sqrt{\frac{1}{N^i}.\sum_{n=1}^{N^i} Ie_n{}^2}. \tag{11}$$

IV. The ARADC Design Flow

From above discussion, it is clear that the ARADC effective resolution is a function of Δa, T_{Timer}, M and I^O. Let us first consider Δa. A generalized modeling of Δa is not straightforward. It depends on the circuit architecture and the technology employed for its implementation [13, 17]. A study on Δa for the Allier's LCADC [8], is made in [13]. Following this work, the proposed design flow is an

extension of the one presented in [8].

Δa mainly occurs because of the process and the mismatch variations, introduced during the circuit fabrication. For the targeted *ENOB*, a design and implementation effort should be made to achieve a minimum Δa for the chosen circuit architecture and technology.

An appropriate value of T_{Timer} can be calculated for input signal PSD (Power Spectral Density) and the obtained Δa [8, 13]. It should be done in such a way that the employed T_{Timer} renders the maximum LCADC SNR_{real} for the obtained Δa.

After deciding values of Δa and T_{Timer}, the next step is to choose appropriate values of M and I^O. Ideally these values should be chosen in such a way that the system SNR_{real} at resampler input and output remains similar.

For a fixed Δa, T_{timer} and I^O the resampled data *SNR* increases up to a certain level with the increase in M [13]. The reason behind is that for any kind of employed interpolation, the upper bound on Ie_n is imposed by q [6]. Here, q is the LCADC. It follows that an increase in M causes a reduction in q, which consequently results into a reduced Ie_n. Increasing M is beneficial up to a certain extent. However, it leads towards a higher circuit area, conversion frequency, power consumption and design complexity [7-9]. Therefore, an optimal M should be chosen, which renders an effective solution for the targeted application.

Similarly, for a fixed Δa, T_{timer} and M the resampled data *SNR* increases up to a certain extent with the increase in I^O [13]. A further increase in I^O accumulates the level-crossing samples time-amplitude pairs uncertainties into the interpolated observation. Thus, reduces the system accuracy. Therefore, an appropriate I^O should be employed, which keeps the system power efficient, while not much affecting the SNR_{real} for the employed Δa, T_{timer} and M.

It follows that, while keeping three parameters among Δa, T_{timer}, M and I^O constant, the ARADC accuracy can be improved to a certain extent by the fourth one. A further fourth parameter error reduction will not significantly improve the ARADC *ENOB*. Here, the limit will be posed by errors due to the remaining three parameters. A further accuracy improvement will require reducing the three remaining parameters error [13].

While following the above discussed criteria, the chosen M should also ensure a proper reconstruction of the acquired signal [7-9, 13, 17]. Moreover, for proper signal capturing the tracking condition should also be respected in the system. It imposes an upper bound on the circuit delay τ_{max}, required to treat one sample point [8].

Following the above discussion the entire ARADC design flow is summarized in Figure 2. Here, shaded blocks distinguish parameters, having direct impact on the ARADC *ENOB*. Once thresholds are established, Δa remains constant [7, 17]. For the given Δa, different LCADC SNR_{real} values can be obtained, within a given range, by tuning T_{Timer}. Moreover, for given Δa, T_{Timer}, and M, different ARADC *ENOB* values can be obtained, within a given range, by varying I^O. It shows the ARADC configurability, means the same circuitry can deliver several *ENOBs*, within a given range, by tuning T_{Timer} and I^O. It shows the possibility of employing the same circuitry for a range of applications.

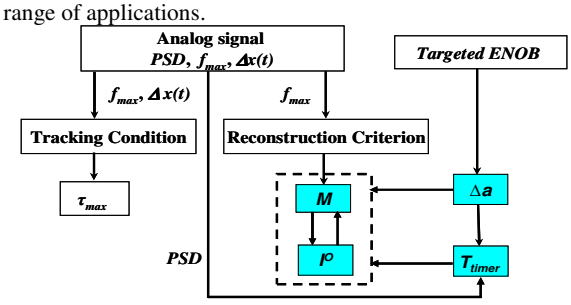

Fig. 2. Design flow of an ARADC.

V. Speech Acquisition as a Case Study

In order to evaluate performances of the ARADC, a speech signal $x(t)$ shown on the top part of Figure 3 is employed. $x(t)$ is bandlimited between [50; 4000] Hz and its total duration is 12 seconds. Its activity is 51.6 % of the total span.

It is known that a good quality speech acquisition requires 13-*ENOB*, while employing a uniform ADC. A similar quality speech can be acquired by using an 8-*ENOB* uniform converter, while employing it with a companding algorithm [20].

The frequency contents of a speech signal vary continuously within the given bandwidth [20]. The proposed system resolution varies for different frequencies within a signal band (cf. Equation 4). The resolution is higher for lower frequencies and vice versa [13]. In order to determine the system resolution for a targeted application, it facilitates characterizing the system with a monotone signal. In [7], Sayiner has argued that for a speech signal, the LCADC effective resolution can be characterized by employing a monotone sinusoid of 568Hz frequency.

In [13], it has been shown that for a set of parameters (Δa=±*0.23%*, T_{timer}=2^{-4}µseconds, M=6 and I^O=1) the ARADC achieves 8-*ENOB*. It is achieved while acquiring a 23000Hz sinusoid. Thus, a better or at least a similar performance can be achieved while dealing with a sinusoid of 568Hz. Therefore, the ARADC with this parameters set is employed along with the mu-law compander, for digitizing the considered speech signal $x(t)$. F_{ref} =16 kHz is chosen, which is a typical speech sampling frequency.

The relevant parts of the non-uniformly sampled signal obtained with the LCADC are selected with the ASA (Activity Selection Algorithm) [5]. It leads to six selected windows (cf. Figure 3). The selected windows parameters are summarised in Table 1.

TABLE1
SUMMARY OF THE SELECTED WINDOWS PARAMETERS

W^i	L^i (Sec.)	Fs^i (Hz)	F_{ref} (Hz)	Frs^i (Hz)	Nr^i (Samples)
1st	1.29	13990	16000	13990	18047
2nd	0.97	21068	16000	16000	15619
3rd	0.55	14898	16000	14898	8173
4th	1.35	12783	16000	12783	17257
5th	0.62	18683	16000	16000	9920
6th	1.42	10487	16000	10487	14881

Table 1, exhibits the interesting features of the ARADC, which are achieved grace of a smart combination of the LCADC, the ASA and the resampler. L^i exhibits the ASA dynamic feature, which is to correlate the window function length with the signal activity. Fs^i represents the sampling frequency adaptation by following the local variations of $x(t)$. Here, the case, Fs^i>F_{ref} holds for the 2^{nd} and the 5^{th} selected windows. However, the opposite is true for the remaining ones. The chosen Frs^i shows the resampling frequency adaptation for W^i. It further adds to the proposed system power efficiency, by avoiding the unnecessary interpolations during the data resampling process. Nr^i shows that how the adjustment of Frs^i avoids the unnecessary samples, delivered at the ARADC output.

In the classical case, if the sampling is performed at F_{ref}, then the whole signal will be sampled at 16000 Hz, regardless of its local variations. Moreover, the windowing process is not able to select only the sampled signal active parts. In addition, the window function length L remains static and is not able to adapt with $x(t)$ local variations. For the studied signal, L=2 seconds will lead to six 2 seconds length windows for the total $x(t)$ span of 12 seconds. The windowed data obtained in the classical case is shown on the bottom part of Figure 3. This static nature results into an increased number of samples delivered at the classical ADC output and so an increased utilization of the system resources compared to the proposed case.

In classical case, a M=8-bit converter along with mu-law compander is employed for acquiring $x(t)$. It delivers 192000 samples for the complete $x(t)$ span. However, for the above discussed set of parameters, the ARADC delivers 83897 samples. It shows that the ARADC delivers 2.3 times less number of samples compared to the classical approach. Around 84 % of this gain is achieved because of the ASA smart features, which is to select only the input signal relevant parts. Remaining 16 % gain is achieved by adapting the resampling frequency according to the input signal local variations.

Note that the considered speech signal activity is 51.6 %, which is more than twice of the activity occurs during a conversational speech [19]. Therefore, while considering a conversational speech, the reduction in number of samples, delivered by the considered ARADC will be greater than or at least equal to 4 times.

The above results confirm that the ARADC can achieve a drastic acquisition activity reduction over the classical one, especially in the case of low activity sporadic signals like electrocardiogram, phonocardiogram, speech, seismic etc.

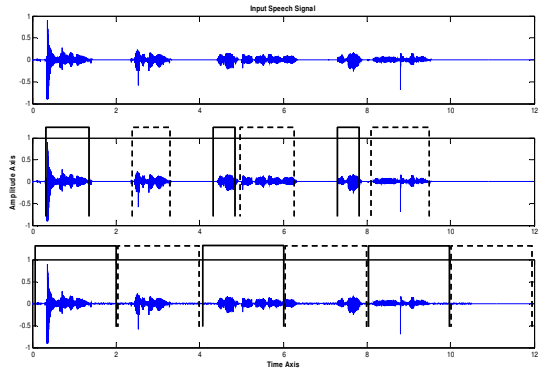

Fig. 3. The input speech signal (top), the selected signal obtained with the ASA (middle) and the windowed signal obtained in the classical case (bottom).

VI. CONCLUSION

A new adaptive rate A/D conversion approach has been devised. The ARADC is especially well suited for the low activity sporadic signals like electrocardiogram, phonocardiogram, speech, seismic, etc. The ARADC design flow has been presented. A trade off between different system parameters is shown. It follows that for a targeted application an appropriate set of parameters (Δa, T_{timer}, M and the I^O) should be found, which provides an attractive trade off between the system power consumption, area, complexity and the delivered output quality, while ensuring the proper signal reconstruction.

The ARADC outperforms compared to the counter classical one. The first advantage is the acquisition efficiency, achieved by acquiring only the relevant signal parts at relevant sampling rates. The second advantage is the configurability, by controlling T_{Timer} and I^O different *ENOB* can be achieved from a single circuit within a given range. These smart features of the ARADC are achieved due to the joint benefits of the LCADC, the ASA and the resampler.

The development of a computer aided tool for finding an optimal set of the ARADC parameters for the targeted application is in progress. The proposed approach employment for other appropriate applications is a prospect.

VII. ACKNOWLEDGEMENT

Authors are thankful to Dr. Laurent Fesquet and to Prof. Marc Renaudin for their fruitful discussions and orientation.

REFERENCES

[1] I. Bilinskis, “Digital alias free signal processing”, John Wiley and Sons, Ltd, 2007.
[2] J.W. Mark and T.D. Todd, “A nonuniform sampling approach to data compression”, IEEE Transactions on Communications, vol. COM-29, pp. 24-32, January 1981.
[3] M. Gretains, “Time-frequency representation based chirp like signal analysis using multiple level crossings”, EUSIPCO’07, pp.2154-2158, September 2007.
[4] K. M. Guan and A.C. Singer. “Opportunistic Sampling by Level-Crossing”, ICASSP’07, pp.1513-1516, April 2007.
[5] S.M. Qaisar et al., “Spectral Analysis of a signal Driven Sampling Scheme”, EUSIPCO’06, September 2006.
[6] S.M. Qaisar et al., “Computationally efficient adaptive rate sampling and filtering”, EUSIPCO’07, pp.2139-2143, September 2007.
[7] N. Sayiner, H.V. Sorensen and T.R. Viswanathan, “A Level-Crossing Sampling Scheme for A/D Conversion”, IEEE Transactions on Circuits and Systems, vol. 43, pp. 335-339, April 1996.
[8] E. Allier, G. Sicard, L. Fesquet and M. Renaudin, “A new class of asynchronous A/D converters based on time quantization”, ASYNC’03, pp.197-205, May 2003.
[9] F. Akopyan, R. Manohar and A.B. Aspel, “A level-crossing flash analog-to-digital converter”, ASYNC’06, pp.12-22, March 2006.
[10] S.M. Qaisar et al., “Computationally efficient adaptive resolution short-time Fourier transform”, EURASIP, RLSP, 2008.
[11] S.M. Qaisar et al., “Adaptive rate filtering for a signal driven sampling scheme”, ICASSP’07, pp.1465-1468, April 2007.
[12] F. Aeschlimann, E. Allier, L. Fesquet and M. Renaudin, “Asynchronous FIR filters, towards a new digital processing chain”, ASYNC’04, pp. 198-206, April 2004.
[13] S.M. Qaisar et al. “Effective Resolution of an Adaptive Rate ADC”, SampTA’09, May 2009.
[14] R.H. Walden, “Analog-to-Digital converter survey and analysis”, IEEE journal on selected areas in communications, vol. 17, No. 4, April 1999.
[15] W. Kester, “Data conversion handbook”, Elsevier/Newnes, 2005, ISBN 0-7506-7841-0.
[16] S. de Waele et al., “Time domain error measures for resampled irregular data”, IEEE Transactions on Instrumentation and Measurements, pp.751-756, 1999.
[17] S.M. Qaisar, “Adaptive Rate Sampling and Processing: A Promising Approach for Computationally Efficient Adaptive Rate Solutions”, PhD dissertation, Grenoble Institute of Technology, France, 2009.
[18] Y. Tsividis, ”Digital signal processing in continuous time: a possibility for avoiding aliasing and reducing quantization error”, ICASSP’04, Canada, 2004.
[19] P.G.Fontolliet, “Systèmes de Télécommunications” Dunod, 1983.
[20] C.W. Brokish and M. Lewis, “A-Law and mu-Law Companding Implementations Using the TMS320C54X”, Texas Instruments, Application Note: SPRA163A.